Efficient nonradiative energy transfer from InGaN/GaN nanopillars to CdSe/ZnS core/shell nanocrystals

Sedat Nizamoglu,[1,a)] Burak Guzelturk,[1] Dae-Woo Jeon,[2] In-Hwan Lee,[2] and Hilmi Volkan Demir[1,3,b)]
[1]*Department of Electrical and Electronics Engineering, Department of Physics, UNAM–National Nanotechnology Research Center, and Institute of Materials Science and Nanotechnology, Bilkent University, Ankara 06800, Turkey*
[2]*School of Advanced Materials Engineering, Research Center of Industrial Technology, Chonbuk National University, Chonju 561-756, Republic of Korea*
[3]*School of Electrical and Electronics Engineering and School of Physical and Mathematical Sciences, Nanyang Technological University, Nanyang Avenue, Singapore 639798*

(Received 5 December 2010; accepted 30 January 2011; published online 20 April 2011)

In this study, we propose and demonstrate efficient electron-hole pair injection from InGaN/GaN multiple quantum well nanopillars (MQW-NPs) to CdSe/ZnS core/shell nanocrystal quantum dots (NQDs) via Förster-type nonradiative energy transfer. For that we hybridize blue-emitting MQW-NPs with red-emitting NQDs and the resultant exciton transfer reaches a maximum rate of $(0.192\ \text{ns})^{-1}$ and a maximum efficiency of 83.0%. By varying the effective bandgap of core/shell NQDs, we conveniently control and tune the excitonic energy transfer rate for these NQD integrated hybrids, and our measured and computed exciton transfer rates are found to be in good agreement for all hybrid cases. © *2011 American Institute of Physics*. [doi:10.1063/1.3562035]

Nanocrystal quantum dots (NQDs) exhibit favorable properties to be exploited for light emitting device applications. They feature size-tuneable effective band gap, strong photoluminescence (PL), high photostability, and easy means of film deposition.[1–3] Electrical current injection into these nanocrystals is possible via using mixture of nanocrystal-polymer composites or hybridization of nanocrystal monolayers into a diode structure.[4,5] However, high potential barriers due to surfactants around NQDs, workfunction mismatch, and charge transport differences between the electrons and the holes limit the efficiency of such electrically driven NQD based devices. Alternatively, Förster-type nonradiative energy transfer (ET) can solve both charge injection and transport problems. In addition, ET has the potential to provide significant energy efficiency enhancement for hybrid light emitting diodes (LEDs).[6–9] Today common LED technology typically makes use of color conversion process involving two recombination steps.[10–12] The first radiative recombination step occurs in multiple quantum wells (MQWs) of the LED, and subsequently, its emitted photons excite its color conversion layer, which in turn luminescences in a second radiative recombination step. ET advantageously eliminates the needs for recombination step in MQWs, subsequent photon extraction from MQWs and optical absorption in the color conversion layer.[13] However, the reported experimental performances in terms of exciton transfer efficiency and percentage of the generated electron-hole pairs undergoing nonradiative ET from QWs to NQDs are commonly limited.

Achermann *et al.*[14] experimentally demonstrated ET pumping of semiconductor nanocrystals using an epitaxial quantum well with a transfer efficiency of 65%. However, in this structure the limitation was that only one single quantum well could contribute to the color conversion through the nonradiative ET process. Furthermore, since the ET coupling scales with d^{-4}, where d is the distance between the QW and NQD monolayer, the topmost layer was required to be extremely thin (typically <10 nm). But, such thinning the top contact layer may undesirably increase the nonradiative carrier losses in the QW and generate other potential problems. As a solution, Chanyawadee *et al.*[15] demonstrated to use the epiwafer having holes with elliptical cross-sections that reach down to the active multiple quantum wells for efficient ET. However, in this structure only 18% of the generated electron-hole pairs experience nonradiative ET with an efficiency of 82%.

Different from the previous studies, we hybridize arrays of InGaN/GaN multiple quantum well nanopillars (MQW-NPs) with CdSe/ZnS core/shell NQDs to enhance Förster-type nonradiative ET. We integrate red-emitting NQDs on blue-emitting MQW-NPs for efficient and fast ET. As a result, an exciton transfer efficiency of 83.0% at a rate of $(0.192\ \text{ns})^{-1}$ is achieved in this hybrid system, while 41% of the generated electron-hole pairs in MQW-NPs undergo nonradiative ET. By further changing the effective bandgap of NQDs, we conveniently adjust the excitonic ET rate for these core/shell NQD integrated hybrids. Also, deriving and computing the exciton transfer rate for all hybrid cases, both calculated and measured ET rates are found to be in good agreement.

InGaN/GaN MQW-NPs are grown and fabricated for efficient exciton donor (see Fig. S1 in Ref. 16). Here one of the main advantages of NP formation is that the MQW-NPs exhibit stronger PL than the planar case.[17,18] In Fig. S2 (in Ref. 16) the PL spectrum of the NP structure is presented, which shows approximately a two-fold PL enhancement. As the acceptor we use trioctylphosphineoxide (TOPO) capped green-, yellow-, and red-emitting CdSe/ZnS core/shell NQDs emitting at 540, 590, and 620 nm. The absorption and PL spectra of these nanocrystals in toluene (measured by Varian fluorometer and spectrometer, respectively) are shown in Fig.

a)Author to whom correspondence should be addressed. Electronic mail: sedatn@ee.bilkent.edu.tr.
b)Electronic mail: volkan@stanfordalumni.org.

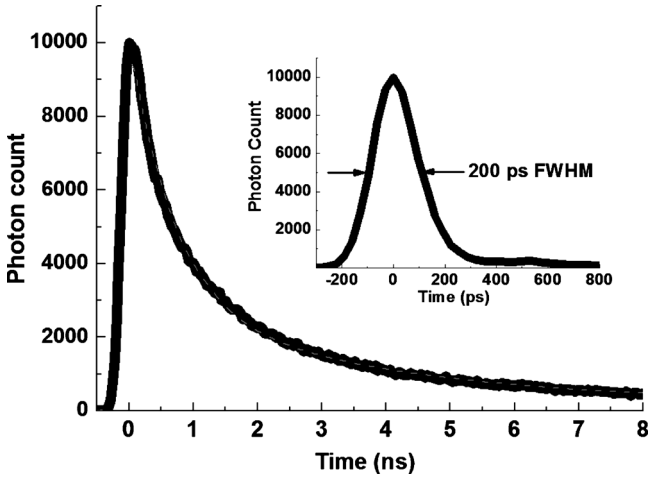

FIG. 1. MQW-NPs PL decay (at λ=450 nm) without NQDs. The dashed lines are the numerical fits as described in text. Inset exhibits IRF and FWHM of our time-resolved system.

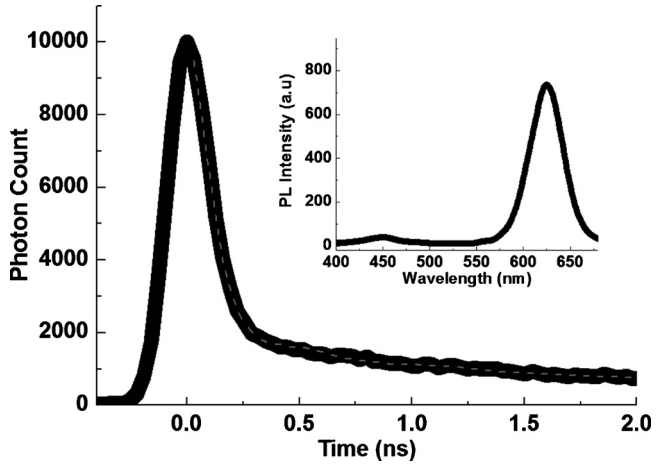

FIG. 2. MQW-NPs PL decay (at λ=450 nm) with red-emitting NQDs. The dashed lines are the numerical fits as described in text. Inset exhibits steady-state PL spectrum of these MQW-NPs with the red-emitting NQDs.

S2 (and further details on NQDs are also provided in Ref. 16). We deposit NQD films on MQW-NPs in a cleanroom of class-100 environment to prevent any contamination on the NP surfaces, which may adversely affect the ET process. We deposit these films by drop-casting on top of the NPs and keep the samples on a hotplate at 100 °C for 1 h to remove excess solvent.

We use a fluorescence lifetime system of FluoTime 200 spectrometer by PicoQuant (Ref. 19) to analyze electron-hole pair transfer dynamics of the hybrid samples (with further details on the system given in Ref. 16). This system achieves an instrument response function (IRF) full-width-at-half-maximum (FWHM) of 200 ps, as shown in the inset of Fig. 1. Because of the finite temporal response of IRF, the exhibited decays are the actual response of NPs convoluted with the IRF response.[20] Thus the time-resolved emission decays may not seem as perfect exponentials. In our analyses, we take this case into account and make numerical fits to the measured decays accordingly. For the case of only NPs shown in Fig. 1, we use Eq. (S1) (provided in Ref. 16), which relates the reference NP PL decay to the, IRF(t), and the PL decay component with a lifetime, τ_{np}, and an amplitude, A. For the case of MQW-NPs hybridized with NQDs presented in Fig. 2, (and also for those depicted in Figs. S3 and S4 in Ref. 16), we use Eq. (S2) in Ref. 16, where τ_{ET} is the nonradiative ET lifetime, because the generated electron-hole pairs close to NQDs (with a distance comparable to or less than 2× Förster radius) make nonradiative ET but those farther away from the NQDs do not.The time-resolved spectroscopy of only MQW-NPs is depicted in Fig. 1, which leads to a decay rate of $(0.944\ \text{ns})^{-1}$ by using Eq. (S1).[16] Strong spectral overlap (J) between the emission of the donor MQW-NPs and the absorption of the acceptor NQDs is important to achieve efficient nonradiative exciton transfer. The spectral overlap is calculated by using Eq. (S3) (given in Ref. 16), which depends on the corrected fluorescence intensity of the donor, $F_D(\lambda)$, and the extinction coefficient of the acceptor, $\varepsilon_A(\lambda)$, at the optical wavelength, λ.[20] The selection of the red-emitting NQDs allows for a strong spectral overlap of $4.421\times10^{16}\ \text{M}^{-1}\,\text{cm}^{-1}\,\text{nm}^4$. In Fig. 2 the time-resolved fluorescence of these MQW-NPs furnished with the red-emitting NQDs at the donor emission wavelength (λ =450 nm) is shown. It is clearly observable that the decay rate of the MQW NPs is increased because of the ET from the NPs to NQDs. To extract the ET rate and the percentage of the electron-hole pairs experiencing nonradiative transfer, we use Eq. (S2). As a result of the numerical analysis, 41% of the generated electron-hole pairs in the MQW-NPs are found to be transferred to the NQDs while the rest of them make recombination in the NPs. Moreover, the nonradiative exciton transfer rate in this hybrid structure is determined to be $(0.192\ \text{ns})^{-1}$. Also using Eq. (S4),[16] an ET efficiency level of 83.0% is found out for this MQW-NP and NQD hybrid sample. Although interspacing between the NPs and NQDs consisting of the ZnS shell (0.6 nm) and TOPO ligands (1.1 nm) decreases the transfer efficiency, the strong spectral overlap results in high ET efficiency. Here it is worth noting that the ZnS shell provides a thick enough potential barrier that prevents the tunneling of carriers so that the NP PL quenching cannot be due to a Dexter-type charge transfer process. Therefore, we can undoubtedly state that the shortening of the lifetime decay of MQW-NPs is as a result of the Förster-type nonradiative ET. In the inset of Fig. 2 the steady-state emission of this hybrid case is presented. The red emission generated by NQDs becomes significantly more dominant with respect to the MQW-NP emission because of the strong ET, which is an important signature of the energy outflow from the NPs and energy inflow into the QDs. It is also an additional fact that the luminescence of NQDs without ET also contributes to the overall emission of NQDs and makes it to be further stronger with respect to the NPs as well.

To further understand and master the excitonic ET process, we vary the spectral overlap between the emission of MQW-NPs and the absorption of NQDs. For that we integrate yellow-emitting CdSe/ZnS core/shell NQDs with InGaN/GaN MQW NPs. The spectral overlap in this case is decreased down to $1.491\times10^{16}\ \text{M}^{-1}\,\text{cm}^{-1}\,\text{nm}^4$. The time-resolved spectroscopy of this hybrid case is shown in Fig. S3 (given in the Ref. 16), for which the decay rate is again observed to increase because of the exciton transfer. According to our numerical fits using Eq. (S2), we find out that 40% of the electron-hole pairs are transferred from MQW-NPs to the yellow-emitting NQDs. The ET rate and efficiency thus correspondingly become slightly lower, which are extracted

to be $(0.237\ \text{ns})^{-1}$ and 79.8%, respectively. Although the spectral overlap decreases for the case of NPs with yellow-emitting NQDs, the ET efficiency does not significantly drop because the distance between NQDs and MQWs decreases, the dot density surrounding MQWs increases and the effective refractive index[20] decreases due to the smaller size of yellow-emitting NQDs in comparison to the red-emitting NQDs. As a result, a high ET efficiency of 79.8% is still maintained. We also incorporate green-emitting NQDs on MQW-NPs, for which the spectral overlap is even further reduced to $4.933\times10^{15}\ \text{M}^{-1}\,\text{cm}^{-1}\,\text{nm}^4$. The time-resolved spectroscopy of this hybrid case with green-emitting NQDs is shown in Fig. S4 (given in Ref. 16). According to our numerical fits, the transfer rate and efficiency decrease to $(0.253\ \text{ns})^{-1}$ and 78.8%, respectively, and the electron-hole pairs undergoing nonradiative ET slightly reduces to 39%. Both in the inset of Figs. S3 and S4, the steady-state emission spectra are shown, and according to them the NQDs emission suppresses the luminescence of MQW-NPs because of the exciton migration from MQW-NPs into NQDs.[16]

We also make computational analyses of exciton transfer rates to further prove the ET process. For that we derive the electron-hole pair transfer formula for our hybrid architectures. According to our model, MQWs transfer their electron-hole pairs to NQD layer at the surface of the NPs. We calculate the expected ET rates by using Eq. (1), which is derived from Eqs. (S5)–(S7) in Ref. 16. For the hybrid case of red-emitting NQDs integrated on MQW-NPs, the spectral overlap (J) is calculated to be 4.421×10^{16}. The interspacing (d) between the center of the nanocrystal and quantum wells in NPs are taken to be 4.0 nm, which consists of 2.3 nm CdSe core radius, 0.6 nm ZnS shell radius, and 1.1 nm TOPO length. The refractive index (n) of 1.934 is estimated by averaging both refractive index of ligands surrounding NQDs as 1.468 and the refractive index of NQD as 2.4.[21] The quantum efficiency of the donor multiple quantum well NPs is 20%. As a result, Förster radius (R_0) corresponds to 5.777 nm. We also know the decay rate of the NPs alone (k_D) to be $(0.944\ \text{ns})^{-1}$ and the dot density (σ) to be $2.100\times10^{12}\ \text{cm}^{-2}$. By plugging all these parameters into Eq. (1) for MQW-NPs with red-emitting NQDs, we obtain an ET rate of $(0.197\ \text{ns})^{-1}$ and this computed value is in good agreement with our measured ET rate of $(0.192\ \text{ns})^{-1}$. Similarly, we also calculated the ET rate for yellow- and green-emitting NQDs on the MQW-NPs and the used parameter values are summarized in Table S1. We obtained the respective ET rates of $(0.230\ \text{ns})^{-1}$ and $(0.248\ \text{ns})^{-1}$, and these are also in good agreement with our measured ET rates of $(0.237\ \text{ns})^{-1}$ and $(0.253\ \text{ns})^{-1}$, respectively. This supports that ET between the NP and NQDs is originated by dipole–dipole interaction, which is in agreement with the Förster model.

$$k_{ET} = \frac{k_D 0.5\pi\sigma R_o^6}{d^4}. \quad (1)$$

In conclusion, we studied nonradiative electron-hole pair migration from InGaN/GaN multiple quantum well Np structures to CdSe/ZnS core/shell NQDs. We observed fast nonradiative exciton transfer from blue-emitting MQW-NPs to red-emitting NQDs at a rate of $(0.192\ \text{ns})^{-1}$. Furthermore, we demonstrated controlled tuning of the excitonic ET rate to $(0.237\ \text{ns})^{-1}$ and $(0.253\ \text{ns})^{-1}$ for the yellow- and green-emitting NQD integrated layers, respectively. In all of these hybrid cases, 41%–39% of the generated electron-hole pairs in the NPs are observed to be transferred to the NQDs. Such hybrid NP architectures decorated with QDs hold great promise for making excitonic devices.

We acknowledge the financial support by ESF European Young Investigator Award (EURYI) program and TUBITAK under the Project Nos. EEEAG 110E010, 109E004, 109E002, and 107E088. H.V.D. acknowledges additional support from the Turkish National Academy of Sciences Distinguished Young Scientist Award (TUBA GEBIP) and NRF RF Fellowship programs.

[1]C. B. Murray, C. R. Kagan, and M. G. Bawendi, Annu. Rev. Mater. Sci. **30**, 545 (2000).
[2]E. Lifshitz, I. Dag, I. Litvin, G. Hodes, S. Gorer, R. Reisfeld, M. Zelner, and H. Minti, Chem. Phys. Lett. **288**, 188 (1998).
[3]S. V. Gaponenko, *Introduction to Nanophotonics* (Cambridge University Press, Cambridge, 2010).
[4]V. L. Colvin, M. C. Schlamp, and A. P. Alivisatos, Nature (London) **370**, 354 (1994).
[5]A. H. Mueller, M. A. Petruska, M. Achermann, D. J. Werder, E. A. Akhadov, D. D. Koleske, M. A. Hoffbauer, and V. I. Klimov, Nano Lett. **5**, 1039 (2005).
[6]V. M. Agranovich, G. C. La Rocca, and F. Bassani, JETP Lett. **66**, 748 (1997).
[7]D. Basko, G. C. La Rocca, F. Bassani, and V. M. Agranovich, Eur. Phys. J. B **8**, 353 (1999).
[8]V. M. Agranovich, D. M. Basko, G. C. La Rocca, and F. Bassani, Synth. Met. **116**, 349 (2001).
[9]S. Nizamoglu, E. Sari, J.-H. Baek, I.-H. Lee, and H. V. Demir, IEEE J. Sel. Top. Quantum Electron. **15**, 1163 (2009).
[10]S. Nakamura and G. Fasol, *The Blue Laser Diode* (Springer, Berlin, 1997).
[11]E. F. Schubert, *Light Emitting Diodes* (Cambridge University Press, New York, 2006).
[12]M. R. Krames, O. B. Shchekin, R. Mueller-Mach, G. O. Mueller, L. Zhou, G. Harbers, and M. G. Craford, J. Disp. Technol. **3**, 160 (2007).
[13]M. Achermann, M. A. Petruska, D. D. Koleske, M. H. Crawford, and V. I. Klimov, Nano Lett. **6**, 1396 (2006).
[14]M. Achermann, M. A. Petruska, S. Kos, D. L. Smith, D. D. Koleske, and V. I. Klimov, Nature (London) **429**, 642 (2004).
[15]S. Chanyawadee, P. G. Lagoudakis, R. T. Harley, M. D. B. Charlton, D. V. Talapin, and S. Lin, Adv. Mater. **22**, 602 (2010).
[16]See supplementary material at http://dx.doi.org/10.1063/1.3562035 for the design, fabrication, and characterization of InGaN/GaN multiple quantum well NP arrays; for Fig. S1 schematic representation of the NP formation, scanning electron microscopy image of the fabricated InGaN/GaN multiple quantum well NPs, and their x-ray diffraction measurement; for Fig. S2 photoluminescence spectra of both planar and nanopillar structures of InGaN/GaN multiple quantum wells, and absorption and emission spectra of CdSe/ZnS core/shell nanocrystal quantum dots; for additional information on NQDs and time-correlated single photon counting (TPSPC) system for PicoHarp 300; for Eq. (S1) fitting only NP sample with a single exponential decay; for Eq. (S2) fitting nanopillars and nanocrystal quantum dots together, for Eq. (S3) giving the spectral overlap J; for Eq. (S4) exhibiting ET efficiency; for Eqs. (S5)–(S7) showing the derivation of the ET rate from multiple quantum well NPs to NQDs; and for Figs. S3 and S4 presenting the time-resolved spectroscopy of multiple quantum well NPs with yellow- and green-emitting NQDs, respectively; Table S1 including parameter values used to calculate ET rate for different samples.
[17]V. Ramesh, A. Kikuchi, K. Kishino, M. Funato, and Y. Kawakami, J. Appl. Phys. **107**, 114303 (2010).
[18]J.-H. Zhu, S.-M. Zhang, X. Sun, D.-G. Zhao, J.-J. Zhu, Z.-S. Liu, D.-S. Jiang, L.-H. Duan, H. Wang, Y.-S. Shi, S.-Y. Liu, and H. Yang, Chin. Phys. Lett. **25**, 3485 (2008).
[19]http://www.picoquant.com/ (accessed Aug 30, 2010).
[20]J. R. Lakowicz, *Principles of Fluorescence Spectroscopy* (Springer, New York, 2006).
[21]L.-W. Wang and A. Zunger, Phys. Rev. B **53**, 9579 (1996).